Anat Embryol (2005) 210: 343–352
DOI 10.1007/s00429-005-0025-5

ORIGINAL ARTICLE

K. Amunts · O. Kedo · M. Kindler · P. Pieperhoff
H. Mohlberg · N.J. Shah · U. Habel · F. Schneider
K. Zilles

# Cytoarchitectonic mapping of the human amygdala, hippocampal region and entorhinal cortex: intersubject variability and probability maps

Published online: 6 October 2005


**Abstract** Probabilistic maps of neocortical areas and subcortical fiber tracts, warped to a common reference brain, have been published using microscopic architectonic parcellations in ten human postmortem brains. The maps have been successfully applied as topographical references for the anatomical localization of activations observed in functional imaging studies. Here, for the first time, we present stereotaxic, probabilistic maps of the hippocampus, the amygdala and the entorhinal cortex and some of their subdivisions. Cytoarchitectonic mapping was performed in serial, cell-body stained histological sections. The positions and the extent of cytoarchitectonically defined structures were traced in digitized histological sections, 3-D reconstructed and warped to the reference space of the MNI single subject brain using both linear and non-linear elastic tools of alignment. The probability maps and volumes of all structures were calculated. The precise localization of the borders of the mapped regions cannot be predicted consistently by macroanatomical landmarks. Many borders, e.g. between the subiculum and entorhinal cortex, subiculum and Cornu ammonis, and amygdala and hippocampus, do not match sulcal landmarks such as the bottom of a sulcus. Only microscopic observation enables the precise localization of the borders of these brain regions. The superposition of the cytoarchitectonic maps in the common spatial reference system shows a considerably lower degree of intersubject variability in size and position of the allocortical structures and nuclei than the previously delineated neocortical areas. For the first time, the present observations provide cytoarchitectonically verified maps of the human amygdala, hippocampus and entorhinal cortex, which take into account the stereotaxic position of the brain structures as well as intersubject variability. We believe that these maps are efficient tools for the precise microstructural localization of fMRI, PET and anatomical MR data, both in healthy and pathologically altered brains.

**Key words** Hippocampus · Amygdala · Entorhinal cortex · Cytoarchitecture · Probabilistic maps · Atlas · Human brain · Allocortex

K. Amunts (✉) · O. Kedo · P. Pieperhoff · H. Mohlberg
N.J. Shah · K. Zilles
Research Center Jülich, IME, 52425 Jülich, Germany
E-mail: k.amunts@fz-juelich.de
Tel.: +49-2461-618307
Fax: +49-2461-611518

U. Habel · F. Schneider · K. Amunts
Department of Psychiatry and Psychotherapy,
RWTH Aachen University, Aachen, Germany

M. Kindler · K. Zilles
C. and O. Vogt Institute of Brain Research,
University of Düsseldorf, Düsseldorf, Germany

F. Schneider · K. Zilles
Brain Imaging Center West, Research Center Jülich, Jülich, Germany

N.J. Shah
Institute of Physics, University of Dortmund,
Dortmund, Germany

## Introduction

The human amygdala, hippocampus and entorhinal cortex are allocortical regions involved in emotional processes, learning and memory. They have been frequently studied using functional imaging techniques (functional magnetic resonance imaging (fMRI) and positron emission tomography (PET)) as well as in vivo brain morphometry using structural MRI.

The amygdala is not a single homogeneous structure but rather represents a complex of many subnuclei. The subnuclei have been described using different parcellation schemes (Heimer et al. 1999). The subnuclei of the amygdala can be identified based on differences in their cytoarchitecture, myeloarchitecture and chemoarchitecture (Brockhaus 1938, 1940). One of the most widely accepted classification schemes distinguishes the superficial (corticoid) amygdaloid nuclei from the centromedial group and the laterobasal complex (Heimer et al. 1999).

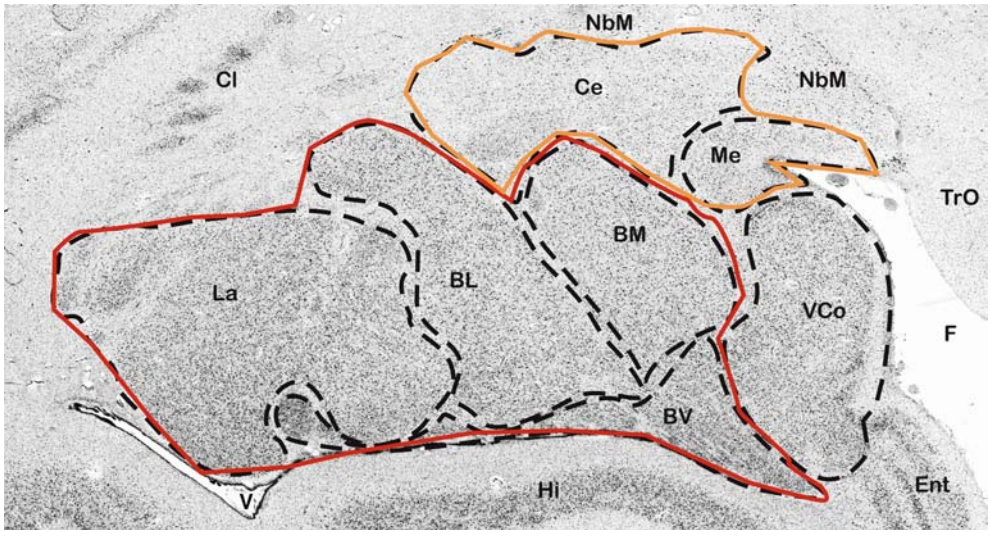


**Fig. 1** Cytoarchitecture of the amygdala and neighboring cortical and subcortical structures in a coronal section of a human postmortem brain. The centromedial nucleus is labelled by an *orange line* and the basolateral complex by a *red line*. The *VCo* belongs to the superficially located part of the amygdala. *BL* basolateral nucleus, *BM* basomedial nucleus, *BV* basoventral nucleus, *Ce* central nucleus, *La* lateral nucleus, *Me* medial nucleus, *VCo* (ventral) cortical nucleus. Neighbouring structures: *Cl* Claustrum, *Ent* entorhinal cortex, *F* endorhinal sulcus, *Hi* hippocampus, *NbM* Nucleus basalis of Meynert, *TrO* Tractus opticus, *V* lateral ventricle

The amygdala has extensive afferent and efferent connections with the diencephalon, the mediofrontal, orbitofrontal and lateral prefrontal cortical regions, hypothalamic nuclei, olfactory brain regions, basal ganglia and the brain stem, whereby many connections are reciprocal (Nieuwenhuys et al. 1988). The amygdala is also strongly connected to the entorhinal cortex and the subiculum. The numerous connections of the amygdala are the structural basis of a large variety of cognitive functions and affective behaviours such as defence, escape, pain, motivation, emotional discrimination, learning and memory (Phelps 2004; Swanson and Petrovich 1998; Ledoux 2000; Aggleton 2000).

Participation of the amygdala, hippocampus and entorhinal cortex in affective functions and dysfunctions has been demonstrated in many studies of the living human brain (Schneider et al. 2000). Morphological and functional imaging studies identified alterations of the amygdala and the hippocampus in schizophrenia (Becker et al. 1996; Bogerts 1997; Heimer 2000; Conrad et al. 1991; van Erp et al. 2004). The activity of the amygdala was decreased in patients with schizophrenia and healthy relatives as compared to healthy controls after experimental induction of sadness (Habel et al. 2004; Schneider et al. 1998). A PET study showed a left-hemispheric decrease of the glucose metabolism in such patients (Nordahl et al. 1996). Several in vivo imaging studies reported hippocampal volume reductions in patients with schizophrenia as compared to healthy volunteers (Nelson et al. 1998; Wright et al. 2000). Morphometric analysis has also shown changes in the entorhinal cortex and hippocampus in Alzheimer's disease (Bobinski et al. 1999; Thompson et al. 2004).

In vivo structural and functional studies analyzing the amygdala, the hippocampal region and/or the entorhinal cortex in normal and pathologically altered brains very often rely on their identification in structural MR images of the individual brain. Most such studies treat the structures as a whole. In some of them, anatomical interpretation is based on the atlas system of Talairach and Tournoux (1988) which shows only very approximate positions of the hippocampus and the amygdala in one hemisphere.

Using in vivo MRI of the hippocampus, a rostral-to-caudal subdivision into head, body and tail has been proposed (Kiefer et al. 2004). Several studies showed differences between the anterior and posterior hippocampal regions in frontal lobe dysfunction (Narr et al. 2004; Schacter and Wagner 1999; Lepage et al. 1998).

The functionally relevant subdivisions into Fascia dentata, subregions of the Cornu ammonis (CA 1–CA 4) and subiculum are, however, beyond the spatial resolution of in vivo MRI using standard protocols. For example, the thickness of the CA regions goes down to less than 1 mm, which is less than the spatial resolution of routine MRI on whole-body, clinical scanners. The same holds true for the subdivision of the amygdala even for coarse parcellations such as the Supraamygdaleum and the Amygdalaeum proprium by Brockhaus (1938). Detailed information on subnuclei of the amygdala is currently not available from in vivo imaging studies (Brierley et al. 2002). Furthermore, the relatively low contrast of the amygdala does not enable an unambiguous delineation from neighbouring regions, e.g. at the border of the cortical nucleus of the amygdala and the neocortex, between the amygdala and the caudate nucleus, and between the amygdala and the hippocampus (Figs. 1, 2). Such information, however, is important, since the different nuclei of the amygdala (and regions of the hippocampus) are segregated not only by their

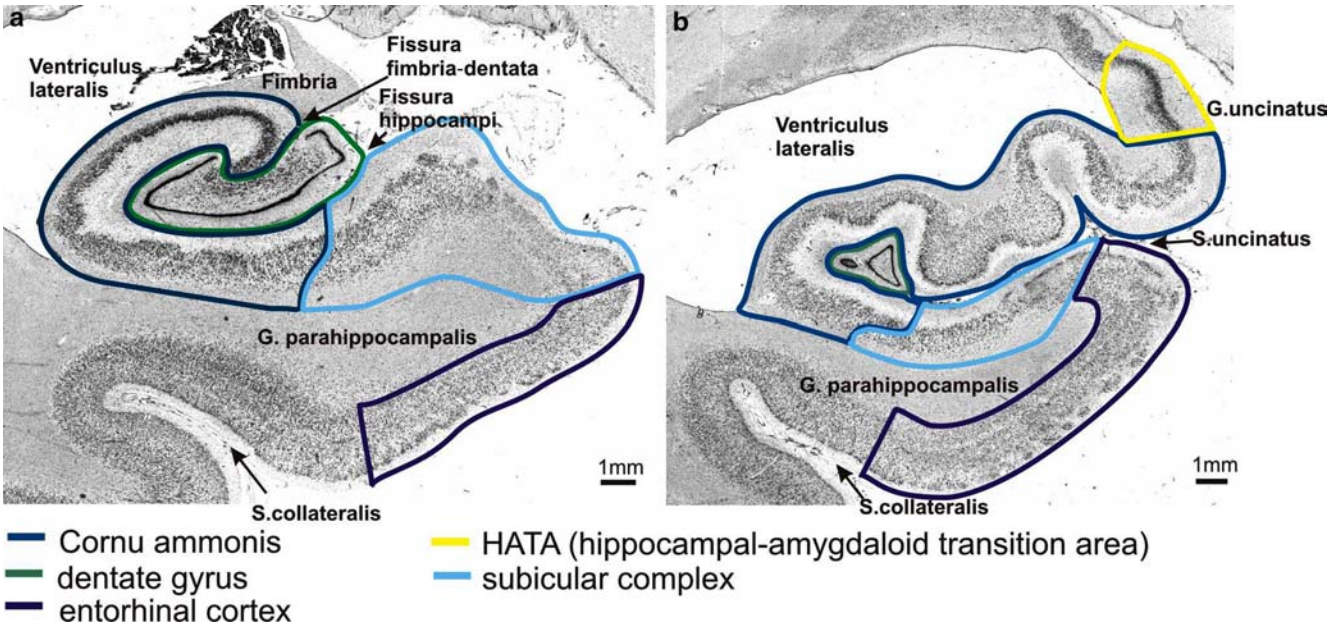


**Fig. 2** Cytoarchitecture of the mesial temporal lobe at the level of the body of the hippocampus (**a**), and its head (**b**). The hippocampus proper with its subdivisions Cornu ammonis, dentate gyrus, the *HATA*, the subicular complex and the entorhinal cortex are labelled by *different colours*. Note that cytoarchitectonic borders of the different subdivisions do not coincide with sulci in most cases

architecture and connectivity, but also by their vulnerability in age-related changes and neuropsychiatric disorders (Harding et al. 1998; Heimer 2000; Irwin et al. 2004; Simic et al. 1997; Narr et al. 2004).

Therefore, we have generated architectonic maps of the Cornu ammonis, the subicular complex, Fascia dentata together with CA4, the hippocampal-amygdaloid transition area (HATA), the amygdala with its centromedial, superficial and laterobasal nuclear groups as well as the entorhinal cortex taking advantage of the high spatial resolution of microscopic techniques. The individual maps were reconstructed in 3D and transferred to a stereotaxic reference space in order to provide a tool for the required detailed localization of future functional and structural MRI data of patients with neuropschiatric disorders and healthy controls.

## Materials and methods

Cytoarchitectonic mapping (Figs. 1, 2) was performed as previously described (Zilles et al. 2002; Amunts and Zilles 2001) in serial coronal sections (thickness: 20 μm, silver staining by Merker (1983) for cell bodies) in both hemispheres of ten postmortem human brains (five males, five females; mean age: 64.9 years, SD = 16.9) with no history of neurological or psychiatric diseases. Brains were taken from body donors in accordance with the guidelines of the Ethics Committee of the University of Düsseldorf. Handedness was unknown. In order to correct for distortions, inevitable during histological processing, the fixed post-mortem brains were placed in a cylindrical container filled with formalin and placed in the headcoil of an MRI scanner. The measurement protocol was carried out on a Siemens 1.5 T scanner (Siemens Medical Systems GmbH, Erlangen, Germany) equipped with a gradient system capable of 25 mT/m; the standard radiofrequency head coil was used for signal reception and transmission of radiofrequency excitation pulses. Images were acquired with a T1-weighted FLASH sequence covering the entire brain (flip angle = 40°, repetition time, TR = 540 ms, echo time TE = 5.5 ms for each image). Spatial resolution was 1×1×1.17 mm. These MR images served as a reference for the 3-D reconstruction of the histological sections and their cytoarchitectonic structures (Schormann and Zilles 1998). The 3-D reconstructions of the histological data sets were calculated on the basis of three original data sets: (i) the MR scan of the fixed brain prior to embedding in paraffin, (ii) the blockfaces of the paraffin blocks which were obtained during histological sectioning, and (iii) the images of the cell-body stained histological sections (Amunts et al. 1999; Schormann and Zilles 1998; Zilles et al. 2002; Henn et al. 1997).

The following structures were identified:

1. Hippocampal formation (Amaral and Insausti 1990).
   - Cornu ammonis (CA1–CA3).
   - Dentate gyrus (DG) including Fascia dentata and CA4 (Duvernoy 1988).
   - Subicular complex (including the prosubiculum, subiculum proper, presubiculum and parasubiculum (Duvernoy 1988; Rosene and van Hoesen 1987).
2. Hippocampal-amygdaloid transition area (HATA), a component of the uncal hippocampal formation (Rosene and van Hoesen 1987).

3. Amygdala (Heimer et al. 1999).
   - Superficial group (includes the anterior amygdaloid area, the amygdalopyriform transition area, the amygdaloid-hippocampal area and the ventral (intermediate, dorsal, ventral) and posterior cortical nuclei).
   - Centromedial group (central nucleus and medial nucleus).
   - Laterobasal group (lateral nucleus, basolateral, basomedial and paralaminar nuclei).
4. Entorhinal cortex (Heinsen et al. 1996; Krimer et al. 1997; Braak 1972).

The borders of these eight structures were interactively traced on images of histological sections (Figs. 1, 2) of the 3-D reconstructed post-mortem brain data sets and registered to standard reference space (see below).

## Volume measurements

The volumes of the structures (Table 1) were calculated based on measurements of the area of the delineated structures in images of the individual histological section using the following formula:

$$V = s \times T \times x \times y \times \sum A_i \times F$$

where $V$ is the volume of the cortical region ($mm^3$), $s$ is the distance between two measured sections (60), $T$ is the thickness of a histological section (0.020 mm), $x$ is the width of a pixel (0.02116 mm), $y$ is the height of a pixel (0.02116 mm), $\Sigma A_i$ is the sum of areas across all $i$ sections evaluated (in pixels) and $F$ is the shrinkage factor of each individual brain.

Areas were measured using the KS400® image analyzing system (Zeiss, Germany). Depending on the extent of each area, 7–20 sections were analyzed per hemisphere and brain.

In order to estimate the true volumes, shrinkage due to histological processing has to be taken into account. Shrinkage differs with respect to age, sex, clinical history, brain size, cause of death, autopsy conditions, histological techniques and other factors (Blinkov and Glezer 1968; Haug 1980; Skullerud 1985; Vierordt 1893). The individual shrinkage factors of the postmortem brains were defined as the ratio between the estimated fresh volume of the brain and its volume after histological processing (histological sections). The fresh volumes were calculated from the fresh weight of the brain and a mean specific density of 1.033 (Kretschmann and Wingert 1971). The volumes of the histological sections were calculated based on area measurements of the brain tissue in the digitized histological sections (resolution of the digitized images: 14.000×12.000 pixels).

## 3-D reconstruction of microscopical structures and generation of probabilistic maps

All cytoarchitectonic structures were 3-D reconstructed, and registered to the stereotaxic space of the MNI reference brain (Collins et al. 1994; Holmes et al. 1998; Evans et al. 1993) using a combination of linear affine transformation, grey level normalization and non-linear, elastic alignment (Henn et al. 1997; Amunts et al. 2004; Mohlberg et al. 2003).

The MNI reference space is a frequently applied reference space in functional imaging, e.g. in the software environment of SPM (http://www.fil.ion.ucl.ac.uk/spm). This reference space, however, is not precisely aligned to the AC–PC line, connecting the anterior with the posterior commissure (Brett et al. 2002). The origin of the system of coordinates of the MNI space is not defined by the upper edge of the anterior commissure. The coordinates in $y$ and $z$ direction of the MNI space do not correspond to distances from the AC–PC line as in Talairach space (Talairach and Tournoux 1988). The anterior commissure, however, is a consistent anatomical landmark, which is easy to identify in routine MR images. Therefore, orientation of MR data with respect to the AC–PC line is well accepted in neurosurgery as well as in many functional imaging studies (Talairach and Tournoux 1988; Roland and Zilles 1994; Hardy et al. 1992). The two spaces, the MNI space and the stereotaxic reference space with the origin at the AC, can easily be transformed into each other. We have used such a transformation in the present study. Consequently, the origins of the data were shifted by a linear affine transformation (translation in $y$ and $z$ plane by 4 and 5 mm, respectively) in such a way that the anterior commissure (at the level of the inter-hemispheric fissure) coincided with the origin of the reference space (= anatomical MNI space, orientation according to the AC–PC plane).

In a final step, probability maps of all structures were calculated. Probability maps indicate the relative fre-

**Table 1** Volumes (in $mm^3$, means with standard deviation, $N = 10$)

| Structure | | Left | Right | Total left | Total right |
|---|---|---|---|---|---|
| Amygdala | Superficial | 334 ± 81 | 319 ± 61 | 1536 ± 286 | 1506 ± 272 |
| | Centromedial | 138 ± 31 | 138 ± 28 | | |
| | Laterobasal | 1063 ± 214 | 1050 ± 219 | | |
| Hippocampus | DG | 700 ± 160 | 705 ± 160 | 4713 ± 1007 | 4884 ± 1087 |
| | CA1-3 | 2174 ± 455 | 2290 ± 494 | | |
| | Subiculum | 1767 ± 454 | 1829 ± 490 | | |
| | HATA | 72 ± 23 | 60 ± 19 | | |
| Entorhinal cortex | | 1745 ± 370 | 1678 ± 309 | | |

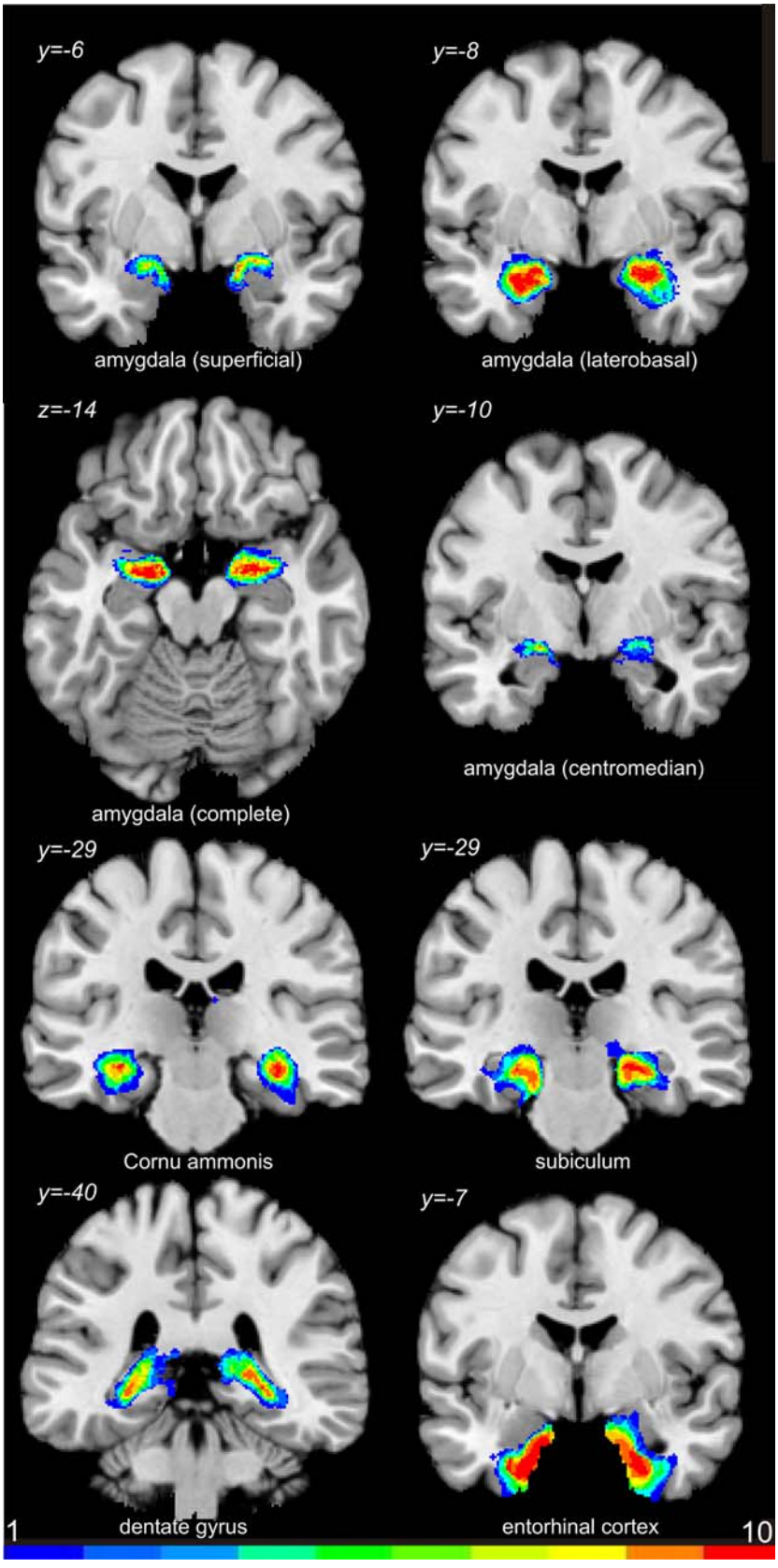


**Fig. 3** Probabilistic maps of the amygdala, hippocampus and entorhinal cortex in anatomical MNI space (*x*, *y* and *z* coordinates indicate distances from the anterior commissure (*AC*) in mm in the medio-lateral, rostro-caudal and dorso-ventral directions, respectively). The left hemisphere is indicated by negative coordinates. Left hemisphere is at the left in the image. The frequency with which an actual anatomical structure was present in the sample of ten brains is colour coded. The scale at the bottom of this figure indicates the degree of overlap in each voxel. *Blue colour* (1) shows that only one brain is represented with its actual structure, *red colour* (10) shows that all ten brains are overlapping

quency with which a cytoarchitectonic structure is present in each voxel of the anatomical MNI space (Fig. 3). Furthermore, a combined stereotaxic map of the mesial temporal lobe was calculated which shows the probabilistic maps of the different brain structures at a common threshold of 40% (Fig. 4).

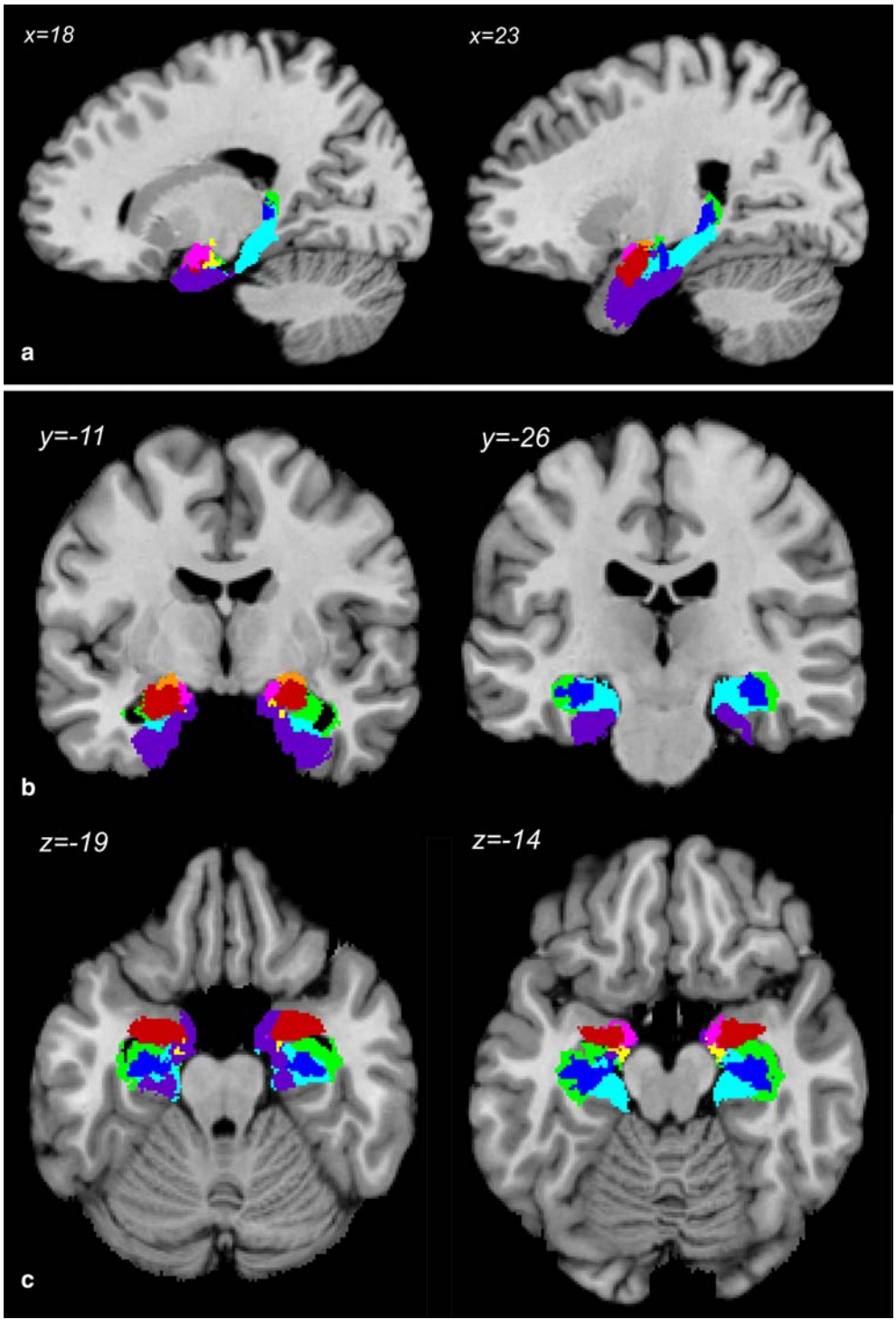


**Fig. 4** Stereotaxic maps of the mesial temporal lobe including the hippocampal formation, subicular complex, entorhinal cortex and amygdala. **a** Sagittal sections, **b** coronal sections, **c** horizontal sections in anatomical MNI space. Only those voxels of the probabilistic maps which overlapped in four or more out of ten brains were labeled. *Orange* centromedial amygdala, *red* basolateral amygala, *magenta* superficial amygdala, *yellow* HATA, *light blue* subiculum, *green* Cornu ammonis, *dark blue* dentate gyrus, *purple* entorhinal cortex

## Results

### Cytoarchitectonic borders and macroanatomical landmarks

#### *Amygdala*

The borders of the amygdala do not coincide, over a large extent, with macroanatomical landmarks whereas other borders fit well. The endorhinal sulcus marks the border to the amygdaloid body for its cortical nucleus (Fig. 1). Parts of ventral borders of the lateral nucleus, the basoventral and basolateral nuclei are indicated by the lateral ventricle (Fig. 1). In contrast, the dorsal borders of the centromedial part of the amygdala (central and medial nuclei) can only be detected at a microscopical level since these two nuclei consist of loosely packed cells (Fig. 1). Such low packing density

of cells makes it difficult or even impossible to distinguish the nuclei from neighbouring structures (Nucleus basalis of Meynert, white matter) at a macroscopical magnification.

*Hippocampal formation and HATA*

The positions of the borders of these structures also cannot be precisely and reliably predicted by macroscopic, anatomical landmarks. The borders between the subiculum and the entorhinal cortex, the subiculum and Cornu ammonis, the amygdala and the HATA region did not coincide with macroscopically visible anatomical landmarks, and are a few examples of this lack of correlation between macroanatomy and cytoarchitecture (Fig. 2).

At the transition between the entorhinal cortex, the hippocampal formation and the amygdala, HATA (Fig. 2b) is inserted between the medial entorhinal cortex, the cortical nucleus of the amygdala, CA1 and the subiculum (Rosene and van Hoesen 1987). The HATA has been interpreted as (the most rostral) part of the uncal hippocampal formation (Rosene and van Hoesen 1987), and corresponds cytoarchitectonically to CA∅ of Stephan (Stephan 1975). The HATA shows a laminar structure, but does not show a Stratum radiatum and Stratum oriens as in CA1. Neurons in HATA are more densely packed and smaller than those of CA1 and the subiculum.

The dentate gyrus with Fascia dentata is a structure, which can clearly be distinguished from the neighbouring Cornu ammonis due to its densely packed band of granular cells. It is often applied as an "internal" landmark of the rostro-caudal extent of the hippocampus. Our cytoarchitectonic analysis showed, however, that HATA reaches more rostral levels than the Fascia dentata (Fig. 4a). It exceeds it by a few millimetres. That is, the Fascia dentata (which is also clearly visible in MRI) is not a precise marker of the rostral extent of the hippocampus. Taking the Fascia as an indicator of the hippocampus would result in an underestimation of the hippocampus with respect to its rostral border.

*Entorhinal cortex*

The entorhinal cortex belongs to the periallocortex. It occupies the parahippocampal gyrus. The entorhinal cortex shows characteristic neuronal islands in layer II, cellular clusters in the superficial part of layer III and a cell-free layer Lamina dissecans (Krimer et al. 1997). Medially, the entorhinal cortex borders to the subiculum whereas isocortical areas adjoin the entorhinal cortex laterally. The lateral border of the entorhinal cortex is roughly marked by the collateral sulcus. The exact position of the lateral border of the entorhinal cortex may vary with respect to the fundus of this sulcus by several millimetres (compare the positions in Figs. 2a and b). In the most rostral sections, however, the lateral border of the entorhinal cortex may also be marked by the rhinal sulcus. The entorhinal cortex may reach the lateral bank of the rhinal cortex if the sulcus is shallow.

Intersubject variability in regional volumes

Table 1 shows the volumes of the subdivisions of the hippocampus and the amygdala. The mean volumes of the whole amygdala ($\pm$SD) are $1536 \pm 286$ mm$^3$ (left hemisphere) and $1526 \pm 272$ mm$^3$ (right hemisphere). The volumes of the hippocampus were 4713 in the left and 4484 mm$^3$ in the right hemisphere. The entorhinal cortex had a volume of 1745 in the left and 1678 mm$^3$ in the right hemisphere (Table 1). The individual volumes varied by a factor of 1.7–2 between the different brains with exception of HATA, which varied by a factor of 3. Interhemispheric and sex related differences in volume were not found.

Intersubject variability in extent and location

The registration of the individual cytoarchitectonic maps of the different brains to the common reference space (anatomical MNI space, see Materials and methods) showed a low degree of intersubject variability in extent and location, and, thus, a high overlap in stereotaxic space (Fig. 3). This was particularly true for the entorhinal cortex, and the laterobasal complex of the amygdala. In contrast, the intersubject variability of HATA was the maximal in the group of analyzed structures (maximal overlap of 6–7 brains in a few voxels).

Based on the probabilistic maps of the delineated structures, combined cytoarchitectonic maps have been calculated (see materials and methods, Fig. 4). These maps show a non-overlapping parcellation of the mesial temporal lobe in the anatomical MNI space. They visualize the spatial relationship of the different structures to each other.

## Discussion and conclusions

The present paper provides for the first time cytoarchitectonically verified maps of the amygdala, hippocampus and entorhinal cortex after normalization in stereotaxic space, which consider and quantify the intersubject variability in extent and location of these structures. Whereas some subcortical nuclei, e.g. the striatum, subthalamic nucleus (Pierantozzi et al. 1999) and a few cortical regions, e.g. the entorhinal, perirhinal and temporopolar cortices, have been reported to be reliably identified on MR scans of the living human brain (Insausti et al. 1998; Blaizot et al. 2004; Pruessner et al. 2002) probabilistic maps based on microscopical

observations are superior in those regions where sulcal landmarks do not reflect cytoarchitectonic boundaries. This is particularly true at the transition of the Cornu ammonis region to the subicular complex, and (ii) in brain regions with low differences between neighbouring regions in contrast (e.g. dorsal and medial borders of the amygdala in structural MR images).

The mapping of the amygdala, the hippocampus and the entorhinal cortex, regions critically involved in neural mechanisms of emotional processing, cognition as well as learning and memory, is important for a reliable localization of these brain functions. Thus, it supports attempts to understand the pathophysiology of neuropsychiatric and neurodegenerative disorders.

Probability maps are presently the only approach if a more fine-grained parcellation is required for an anatomical localization of functional imaging data, e.g. with respect to delineations of the subnuclei of the amygdala. Such finer parcellation schemes will play an increasing role with further development of the spatial resolution of MRI, considering that the subnuclei of the amygdala differ in function, architecture and connectivity (Pikkarainen and Pitkänen 2001; Pitkänen et al. 2002; Heimer et al. 1999; Bozkurt et al. 2001). They also differ with respect to their involvement in brain pathology. For example, it has been shown that a proportion of the Lewy bodies-containing neurones in the basolateral nucleus of patients with Parkinson's disease is nearly doubled in cases that exhibited visual hallucinations, suggesting that neuronal dysfunction in this particular subnucleus contributes to this late clinical feature, whereas other subnuclei seem to be unchanged (Harding et al. 2002).

A differentiation between the subnuclei of the amygdala in routine MRI is not feasible because of its relatively low spatial resolution and low contrast. As a consequence, volumes of interest in the amygdala have often been defined not based on its boundaries, but using geometrical structures, e.g. spherical volumes of interest (Heiss et al. 2004). Such geometrically defined volumes of interest, however, include unpredictable portions of neighbouring tissue, including the white substance and isocortical areas.

The intersubject variability in volume of the allocortical region structures was found to be considerably lower than that of previously studied isocortical areas, e.g. areas 44 and 45 of Broca's region (Amunts et al. 1999). The volumes of these two areas differed by a factor of up to 7 when individual shrinkage was considered whereas factors of up to 2 were observed for the allocortical region of the present study. The HATA showed the maximal variability in volumes (factor 3). This high variability in volume as well as the low absolute volume of HATA resulted in a relatively low overlap in the probabilistic cytoarchitectonic map.

The low variability of the amygdala, hippocampus and entorhinal cortex may be a characteristic aspect of phylogenetically older structures as compared to neo-(iso-) cortical areas. Since the probabilistic maps of the allocortical (and periallocortical) brain regions show such a high overlap in the common reference space, the probability maps are precise and efficient tools for the anatomical localization of functional imaging data from both healthy human subjects and neuropsychiatric patients. They can also be applied as microscopically defined regions of interest for the precise topographical analysis of receptor PET studies as shown by Hurlemann et al. in this volume (Hurlemann et al. 2005).

The probabilistic maps are available at http://www.fz-juelich.de/ime/ime_start/ and http://www.bic.mni.mcgill.ca/. They can easily be applied using a toolbox developed for the application of cytoarchitectonic probabilistic maps as an option integrated in the SPM software (Eickhoff et al. 2005). The toolbox can also be downloaded at http://www.fz-juelich.de/ime/ime_start/.

**Acknowledgments** This Human Brain Project/Neuroinformatics research is funded by the National Institute of Biomedical Imaging and Bioengineering, the National Institute of Neurological Disorders and Stroke, and the National Institute of Mental Health. Further support by Deutsche Forschungsgemeinschaft (Schn 362/13-1 and 13-2), the BMBF (BMBF 01GO0104), Brain Imaging Center West (BMBF 01GO0204) and the Helmholtz Gemeinschaft (VH-NG-012) is gratefully acknowledged.

## References

Aggleton JP (2000) The amygdala: a functional analysis. Oxford University Press, Oxford

Amaral DG, Insausti R (1990) Hippocampal formation. In: Paxinos G (ed) The Human Nervous System. Academic Press, San Diego, CA, pp 755

Amunts K, Schleicher A, Bürgel U, Mohlberg H, Uylings HBM, Zilles K (1999) Broca's region revisited: cytoarchitecture and intersubject variability. J Comp Neurol 412:319–341

Amunts K, Weiss PH, Mohlberg H, Pieperhoff P, Gurd J, Shah JN, Marshall CJ, Fink GR, Zilles K (2004) Analysis of the neural mechanisms underlying verbal fluency in cytoarchitectonically defined stereotaxic space—the role of Brodmann's areas 44 and 45. Neuroimage 22:42–56

Amunts K, Zilles K (2001) Advances in cytoarchitectonic mapping of the human cerebral cortex. In: Naidich TP, Yousry TA, Mathews VP (eds) Neuroimaging clinics of North America Anatomic basis of functional MR imaging. Harcourt, Philadelphia, pp 151–169

Becker T, Elmer K, Schneider F, Grodd W, Bartels M, Heckers S, Beckmann H (1996) Confirmation of reduced temporal limbic structure volume on magnetic resonance imaging in male patients with schizophrenia. Psychiatry Res 67:135–143

Blaizot X, Martinez-Marcos A, del Mar Arroyo-Jimenez M, Marcos P, Artacho-Pérula E, Munoz M, Chavoix C, Insausti R (2004) The parahippocampal gyrus in the baboon: Anatomical, cytoarchitectonic and magnetic resonance imaging (MRI) studies. Cereb Cortex 14:231–246

Blinkov SM, Glezer II (1968) Das Zentralnervensystem in Zahlen und Tabellen. Fischer, Jena

Bobinski M, deLeon MJ, Convit A, DeSanti S, Wegiel J, Tarshish CY, Saint Louis LA, Wisniewski HM (1999) MRI of entorhinal cortex in mild Alzehimer's disease. The Lancet 353:38–40

Bogerts B (1997) The temporolimbic system theory of positive schizophrenic symptoms. Schizophr Bull 23:423–434

Bozkurt A, Kamper L, Stephan KE, Kötter R (2001) Organization of primate amygdalo-prefrontal projections. Neurocomputing 38–40:1135–1140

Braak H (1972) Zur Pigmentarchitektonik der Großhirnrinde des Menschen I Regio entorhinalis. Z Zellforsch 127:407–438
Brett M, Johnsrude IS, Owen AM (2002) The problem of functional localization in the human brain. Nat Rev Neurosci 3:243–249
Brierley B, Shaw P, David AS (2002) The human amygdala: a systematic review and meta-analysis of volumetric magnetic resonance imaging. Brain Res Rev 39:84–105
Brockhaus H (1938) Zur normalen und pathologischen Anatomie des Mandelkerngebietes. J Psychol Neurol 49:1–136
Brockhaus H (1940) Die Cyto- und Myeloarchitektonik des Cortex claustralis und des Claustrum beim Menschen. J Psychiat Neurol 49:249–348
Collins DL, Neelin P, Peters TM, Evans AC (1994) Automatic 3D intersubject registration of MR volumetric data in standardized Talairach space. J Comp Ass Tomog 18:192–205
Conrad AJ, Abebe T, Austin R, Forsythe S, Scheibel AB (1991) Hippocampal pyramidal cell disarray in schizophrenia as a bilateral phenomenon. Arch Gen Psychiatry 48:413–417
Duvernoy H (1988) The Human Hippocampus. An Atlas of Applied Anatomy. J.F. Bergmann Verlag, München
Eickhoff S, Stephan KE, Mohlberg H, Grefkes C, Fink GR, Amunts K, Zilles K (2005) A new SPM toolbox for combining probabilistic maps and functional imaging data. Neuroimage 25:1325–1335
Evans AC, Collins DL, Mills SR, Brown ED, Kelly RL, Peters TM (1993) 3D statistical neuroanatomical models from 305 MRI volumes. Proceedings of the IEEE-NSS-M1 Symposium, pp 1813–1817
Habel U, Klein M, Shah NJ, Toni I, Zilles K, Falkai P, Schneider F (2004) Genetic load on amygdala hypofunction during sadness in nonaffected brothers of schizophrenia patients. Am J Psychiatry 161:1806–1813
Harding AJ, Halliday GM, Kril JJ (1998) Variation in hippocampal neuron number with age and brain volume. Cereb Cortex 8:710–718
Harding AJ, Stimson E, Henderson JM, Halliday GM (2002) Clinical correlates of selective pathology in the amygdala of patients with Parkinson's disease. Brain 125:2431–2445
Hardy T, Brynildson LR, Gray YG, Spurlock D (1992) Three-dimensional whole-brain mapping. Stereotact Funct Neurosurg 58:143
Haug H (1980) Die Abhängigkeit der Einbettungsschrumpfung des Gehirngewebes vom Lebensalter. Verh Anat Ges 74:699–700
Heimer L (2000) Basal forebrain in the context of schizophrenia. Brain Res Rev 31:205–235
Heimer L, de Olmos JS, Alheid GF, Pearson J, Sakamoto N, Shinoda K, Marksteiner J, Switzer RC (1999) The human basal forebrain Part II The primate nervous system, Part III. Elsevier, pp 57–226
Heinsen H, Gössmann E, Rüb U, Eisenmenger W, Bauer M, Ulmar G, Bethke B, Schüler M, Schmitt H-P, Götz M, Lockermann U, Püschel K (1996) Variability in the human entorhinal region may confound neuropsychiatric diagnoses. Acta Anat 157:226–237
Heiss WD, Habedank B, Klein JC, Herholz K, Wienhard K, Lenox M, Nutt R (2004) Metabolic rates in small brain nuclei determined by high-resolution PET. J Nucl Med 45:1811–1815
Henn S, Schormann T, Engler K, Zilles K, Witsch K (1997) Elastische Anpassung in der digitalen Bildverarbeitung auf mehreren Auflösungsstufen mit Hilfe von Mehrgitterverfahren. In: Paulus E, Wahl FM (eds) Mustererkennung. Springer, Berlin, pp 392–399
Holmes CJ, Hoge R, Collins L, Woods R, Toga AW, Evans AC (1998) Enhancement of MR images using registration for signal averaging. J Comp Ass Tomog 22:324–333
Hurlemann R, Matusch A, Eickhoff S, Palomero-Gallagher N, Meyer PT, Boy C, Maier W, Zilles K, Amunts K, Bauer A (2005) Analysis of neuroreceptor PET data based on cytoarchitectonic maximum probability maps—a feasibility study. Anat Embryol this volume
Insausti R, Juottonen K, Soininen H, Insausti AM, Partanen K, Vainio P, Laakso MP, Pitkänen A (1998) MR volumetric analysis of the human entorhinal, perirhinal, and temporopolar cortices. Am J Neurorad 19:659–671
Irwin W, Anderle MJ, Abercrombie HC, Schaefer SM, Kalin NH, Davidson RJ (2004) Amygdalar interhemispheric functional connectivity differs between the non-depressed and depressed human brain. Neuroimage 21:674–686
Kiefer C, Slotboom J, Buri C, Gralla J, Remonda L, Dierks T, Strik WK, Schroth G, Kalus P (2004) Differentiating hippocampal subregions by means of quantitative magnetization transfer and relaxometry: preliminary results. Neuroimage 23:1093–1099
Kretschmann H-J, Wingert F (1971) Computeranwendungen bei Wachstumsproblemen in Biologie und Medizin. Springer, Berlin Heidelberg New York
Krimer LS, Hyde TM, Herman MM, Saunders RC (1997) The entorhinal cortex: an examination of cyto- and myeloarchitectonic organization in humans. Cereb Cortex 7:722–731
Ledoux JE (2000) The amygdala and emotion: a view through fear. In: Aggleton JP (ed) The amygdala. A functional analysis. Oxford University Press, Oxford, pp 289–310
Lepage M, Habib R, Tulving E (1998) Hippocampal PET activations of memory encoding and retrieval: the HIPER model. Hippocampus 8:313–322
Merker B (1983) Silver staining of cell bodies by means of physical development. J Neurosc Meth 9:235–241
Mohlberg H, Lerch J, Amunts K, Evans AC, Zilles K (2003) Probabilistic cytoarchitectonic maps transformed into MNI space. Neuroimage CD rom: Ninths international conference on functional mapping of the human brain, New York
Narr KL, Thompson PM, Szeszko P, Robinson D, Jang S, Woods RP, Kim S, Hayashi KM, Asunction D, Toga AW, Bilder RM (2004) Regional specificity of hippocampal volume reductions in first-episode schizophrenia. Neuroimage 21:1563–1575
Nelson MD, Saykin AJ, Flashman LA, Riordan HJ (1998) Hippocampal volume reduction in schizophrenia as assessed by magnetic resonance imaging: a meta-analytic study. Arch Gen Psychiatry 55:433–440
Nieuwenhuys R, Voogt J, van Huijzen C, Lange W (1988) The human central nervous system. A synposis and atlas. Springer, Berlin Heidelberg New York
Nordahl TE, Kusubov N, Carter C, Salamat S, Cummings AM, O'Shora-Celaya L, Eberling J, Robertson L, Huesman RH, Jagust W, Budinger TF (1996) Temporal lobe metabolic differences in medication-free outpatients with schizophrenia via the PET-600. Neuropsychopharmacol 15:541–554
Phelps EA (2004) Human emotion and memory: interactions of the amygdala and hippocampal complex. Curr Opin Neurobiol 14:198–202
Pierantozzi M, Mazzone P, Bassi A, Rossini PM, Peppe A, Altibrandi MG, Stefani A, Bernardi G, Stanzione P (1999) The effect of deep brain stimulation on the frontal N30 component of somatosensory evoked potentials in advanced Parkinson's disease patients. Clin Neurophysiol 110:1700–1707
Pikkarainen M, Pitkänen A (2001) Projections from the lateral, basal and accessory basal nuclei of the amygdala to the perirhinal and postrhinal cortices in rat. Cereb Cortex 11:1064–1082
Pitkänen A, Kelly JL, Amaral DG (2002) Projections from the lateral, basal, and accessory basal nuclei of the amygdala to the entorhinal cortex in the macaque monkey. Hippocampus 12:186–205
Pruessner JC, Köhler S, Crane J, Pruessner M, Lord C, Byrne A, Kabani N, Collins DL, Evans AC (2002) Volumetry of temporopolar, perirhinal, entorhinal and parahippocampal cortex from high-resolution MR images: Considering the variability of the collateral sulcus. Cereb Cortex 12:1342–1353
Roland PE, Zilles K (1994) Brain atlases—a new research tool. Trends Neurosci 17:458–467

Rosene DL, van Hoesen GW (1987) The hippocampal formation of the primate brain. A review of some comparative aspects of cytoarchitecture and connections. In: Jones EG, Peters A (eds) Further aspects of cortical function, including hippocampus. Plenum, New York, pp 345–456

Schacter DL, Wagner AD (1999) Medial temporal lobe activations in fMRI and PET studies of episodic encoding and retrieval. Hippocampus 9:7–24

Schneider F, Weiss U, Kessler C, Salloum JB, Posse S, Grodd W, Müller-Gärtner H-W (1998) Differential amygdala activation in schizophrenia during sadness. Schizophr Res 34:133–142

Schormann T, Zilles K (1998) Three-dimensional linear and non-linear transformations: an integration of light microscopical and MRI data. Hum Brain Mapp 6:339–347

Simic G, Kostovic I, Winblad B, Bogdanovic N (1997) Volume and number of neurons of the human hippocampal formation in normal aging and Alzheimer disease. J Comp Neurol 379:482–494

Skullerud K (1985) Variations in the size of the human brain. Acta Neurol Scand 71:1–94

Stephan H (1975) Allocortex. In: Bargmann W (ed) Handbuch der mikroskopischen Anatomie des Menschen. Springer-Verlag, Berlin Heidelberg New York, pp 339–401

Swanson LW, Petrovich GD (1998) What is the amygdala? Trends Neurosci 21:323–331

Talairach J, Tournoux P (1988) Coplanar stereotaxic atlas of the human brain. Thieme, Stuttgart

Thompson PM, Hayashi KM, de Zubicaray GI, Janke AL, Rose SE, Semple J, Hong MS, Herman DH, Gravano D, Doddrell DM, Toga AW (2004) Mapping hippocampal and ventricular change in Alzheimer disease. Neuroimage 22:1754–1766

van Erp TGM, Saleh PA, Huttunen M, Lonnqvist J, Kaprio J, Salonen O, Valanne L, Poutanen VP, Standerskjold-Nordenstam CG, Cannon TD (2004) Hippocampal volumes in schizophrenic twins. Arch Gen Psych 61:346–353

Vierordt H (1893) Anatomische, physiologische und physikalische Daten und Tabellen zum Gebrauch für Mediziner. Fischer Verlag, Jena

Wright IC, Rabe-Hesketh S, Woodruff PWR, David AS, Murray RM, Bullmore ET (2000) Meta-Analysis of regional brain volumes in schizophrenia. Am J Psychiatry 157:16–25

Zilles K, Schleicher A, Palomero-Gallagher N, Amunts K (2002) Quantitative analysis of cyto- and receptor architecture of the human brain. In: Mazziotta JC, Toga A (eds) Brain mapping: the methods. Elsevier, Amsterdam, pp 573–602